03

The influence of the noise with different spectra on the stability of the flows with rotation

© D.Yu. Zhilenko, O.E. Krivonosova

Institute of Mechanics of Lomonosov Moscow State University, Moscow, Russia
E-mail: jilenko@imec.msu.ru

Received January 31, 2025
Revised April 11, 2025
Accepted April 11, 2025

The effect of two types of noise with different spectra on the stability of viscous incompressible fluid flows in a rotating spherical layer is studied numerically. The noise is introduced into the flow by adding time random fluctuations with zero mean value to the constant mean rotational velocity of the inner sphere. The instability in the form of Taylor vortices is considered. It is found that, for equal amplitudes, different values of the stability limit correspond to distinct noise spectra.

Keywords: noise, instability control, spherical Couette flow.

DOI: 10.61011/TPL.2025.07.61432.20271

Flows in nature and technical systems are usually subject to the influence of external noise [1]. Noise may also be used in extraction of energy from wave and wind flows [2]. The slope of the noise spectrum in logarithmic coordinates (see, e.g., Fig. 1) is commonly represented as $1/f^{\alpha}$; in natural systems, random fluctuations in time are often approximated by „colored" noise [3,4] with a range of variation of $0 < \alpha < 2$ [5]. Such noise may induce bifurcations and transitions to chaos in dynamic systems [6,7]. In a spherical Couette flow (SCF), which is the flow of a viscous incompressible fluid between coaxially located spheres that is driven by rotation of the boundaries, the addition of noise with equal amplitudes but different types of spectra leads to the generation of mean flows of different intensities [8,9]. If white noise with $\alpha = 0$ [10,11] is added, the generation of mean flows in an STC is accompanied by a reduction of the values of critical Reynolds numbers corresponding to the stability limit. The issue of influence of noise with $\alpha \neq 0$ on the position of the stability limit of flows in an STC has not been discussed in [8,9] and remains uninvestigated. This is the reason why the present study is aimed at clarifying this phenomenon. The instability of the so-called primary flow in a thin spherical layer $\delta = (r_2 - r_1)/r_1 = 0.11$, where r_1 and r_2 are the radii of the inner and outer boundaries, respectively, is examined. It has already been studied extensively under stationary boundary conditions both experimentally and numerically [12,13]. Only meridional circulation is observed before the loss of stability in the meridional plane of flow from the pole to the equator. After the loss of stability, a secondary flow is formed. Meridional circulation in it is driven away from the equator by Taylor vortices that are symmetrical relative to the axis of rotation and the plane of the equator. The conditions of their formation were studied both in the case of stationary rotation and with periodic modulation of the rotation velocity [14–16]. Isothermal flows of a viscous incompressible fluid are characterized by the Navier–Stokes and continuity equations

$$\frac{\partial \mathbf{U}}{\partial t} = \mathbf{U} \times \operatorname{rot} \mathbf{U} - \operatorname{grad}\left(\frac{p}{\rho} + \frac{\mathbf{U}^2}{2}\right) - \nu \operatorname{rotrot} \mathbf{U}, \ \operatorname{div} \mathbf{U} = 0,$$

where $\mathbf{U}$ is the velocity field, p is pressure, ρ is density, and ν is the kinematic viscosity of the fluid in a layer. No-slip and impermeability conditions are set at the layer boundaries; they are written below in a spherical coordinate system with radial (r), polar (θ), and azimuthal (φ) directions:

$$u_{\varphi}(r = r_k) = \Omega_k(t) r_k \sin\theta,$$

$$u_r(r = r_k) = 0, \quad u_{\theta}(r = r_k) = 0, \quad k = 1, 2,$$

$k = 1$ — inner sphere; $k = 2$ — outer sphere; u_{φ}, u_r, and u_{θ} — azimuthal, radial, and polar components of velocity, respectively; and Ω_1 and Ω_2 — angular velocities of rotation of the boundaries. The numerical solution method is based on a finite-difference scheme of discretization of the Navier–Stokes equations in space and a semi-implicit third-order Runge–Kutta scheme for integration over time [17,18]. Calculations were carried out with dimensional parameters that correspond closely to the experimental conditions [12]: $\nu = 5 \cdot 10^{-5}\,\mathrm{m^2/s}$, $r_2 = 0.15\,\mathrm{m}$, and $r_1 = 0.1351\,\mathrm{m}$. The total number of nodes was $5.4 \cdot 10^3$ for two-dimensional (2D) calculations with symmetry conditions relative to the rotation axis and the equatorial plane and $8.64 \cdot 10^4$ for three-dimensional (3D) calculations lacking the above symmetry conditions. In 2D calculations, spatial discretization was performed with a reduction in cell size along r near the boundaries; in 3D calculations, the cell size decreased not only along r near the boundaries, but also along θ near the equator. The corresponding ratio of the maximum cell size to the minimum one was 4 and 2 in these two scenarios. Depending on the Reynolds number, 6–9 grid points were

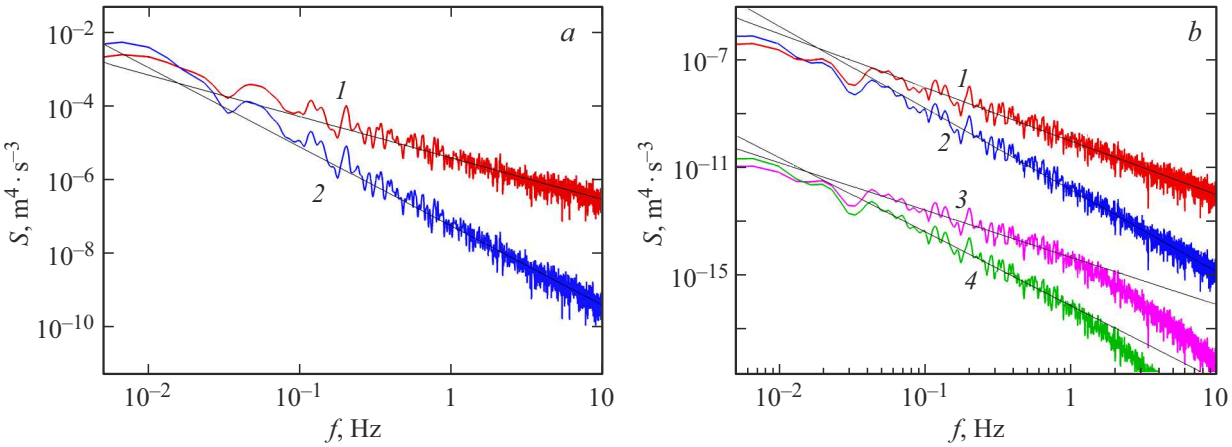

Figure 1. *a* — Spectra of rotation velocity fluctuations. *1* — With slope $\alpha = 1$; *2* — with slope $\alpha = 2$. Black straight lines represent the results of approximation of spectra. *b* — Spectra of fluctuations of kinetic energy components: E_φ $(1,2)$, E_ψ $(3,4)$; $\alpha = 1$ $(1,3)$ and 2 $(2,4)$. $N = 0.06$, $\mathrm{Re}_1 = 1000$.

positioned in the boundary layer, which is sufficient for this layer to be resolved. The convergence of results of 2D calculations at different numbers of computational grid points is presented the table.

Here,

$$K_\varphi = E_\varphi/(\Omega_1 r_1)^2, \quad K_\psi = E_\psi/(\Omega_1 r_1)^2,$$

$$E_\varphi = \int u_\varphi^2(r,\theta,t), \quad E_\psi = \int \left(u_r^2(r,\theta,t) + u_\theta^2(r,\theta,t)\right),$$

E_φ and E_ψ are the azimuthal and meridional components of kinetic energy of flow, respectively, and K_φ and K_ψ are their normalized values. Nonstationary flows driven by rotation of the inner boundary $\Omega(t_j) = \Omega_0 + Nrn(j)$ were investigated; the outer sphere was stationary. The value of average angular velocity Ω_0 corresponded to Reynolds numbers $\mathrm{Re}_1 = \Omega_0 r_1^2/\nu$ varying from 1000 to 1500, N is the noise amplitude, $N = \frac{1}{\Omega_0}\sqrt{\frac{1}{K-1}\sum_{j=1}^{K}\left(\Omega(t_j)-\Omega_0\right)^2}$, $rn(j)$ is a pseudo-random number from a sequence with length K, a standard normal distribution, and zero mean, and j counts the number of time steps. The chosen constant time step $\Delta t = 0.01$ s provided a total of 153–229 time steps in a single revolution of the sphere, $K = 30\,000$. The algorithm [17,18] allows one to control the step size in the process of calculations, but, having performed preliminary calculations, we chose such a value of Δt at which step control did not change its magnitude. A constant Δt value provides an opportunity to preserve the specified values of the spectrum slope and/or noise amplitude in calculations. The duration of each calculation scenario with noise is $600\,\mathrm{s} = 2K\Delta t$. Within the first 300 s, the system reaches a statistically steady state; average values are calculated based on the data obtained in the next 300 s. The results of calculations without noise performed for at least 500 s served as the initial data for calculations with noise. Two types of noise with spectrum slopes $\alpha = 1$ and 2 were used; the same sequence of random numbers was used in calculations with one value of α. As in [9], the sequence of numbers rn was calculated for the chosen spectrum type in advance. Methods for obtaining such sequences were discussed, e. g., in [5].

Dependence of the normalized values of azimuthal (K_φ) and meridional (K_ψ) components of kinetic energy of flow on number G of computational grid nodes in 2D calculations ($\mathrm{Re}_1 = 1000$, $N = 0.06$, and $\alpha = 2$)

$G \cdot 10^{-3}$	K_φ	K_ψ
0.864	0.325188	0.000935
3.456	0.325133	0.000925
4.374	0.325118	0.000922
5.400	0.325108	0.000920
6.144	0.325103	0.000919

In the presence of noise, the flow becomes nonstationary in time, but remains symmetrical with respect to the equator and the axis of rotation [9]. Let us first consider the properties of nonstationary stable flows without Taylor vortices. Figure 1 shows the spectra of $\Omega(t)$, $E_\varphi(t)$, and $E_\psi(t)$ obtained in 2D calculations with different α values. Just as in the case of co-directional rotation of spherical boundaries in wide layers [9], the slope of spectra $\Omega(t)$ α is lower than the slope of spectra $E_\varphi(t)$ α_φ; with the examined values of α, relation $\alpha_\varphi - \alpha \sim 1$ is satisfied (Fig. 1, *a*). In contrast to [9], the slope of spectra $E_\psi(t)$ α_ψ at frequencies below 1 Hz depends on α: $\alpha_\psi - \alpha \sim 0.77$ (Fig. 1, *b*). The addition of noise leads to the generation of mean flows [8–10]. We will examined it using the example of variation of relative azimuthal flow velocity $V = u_{\varphi N}/u_\varphi$, where $u_{\varphi N}$ is the azimuthal flow velocity with noise. The distribution of V in the meridional plane of stable flow is shown in Fig. 2. It is evident that the V distributions corresponding to $\alpha = 1$ and 2 are qualitatively

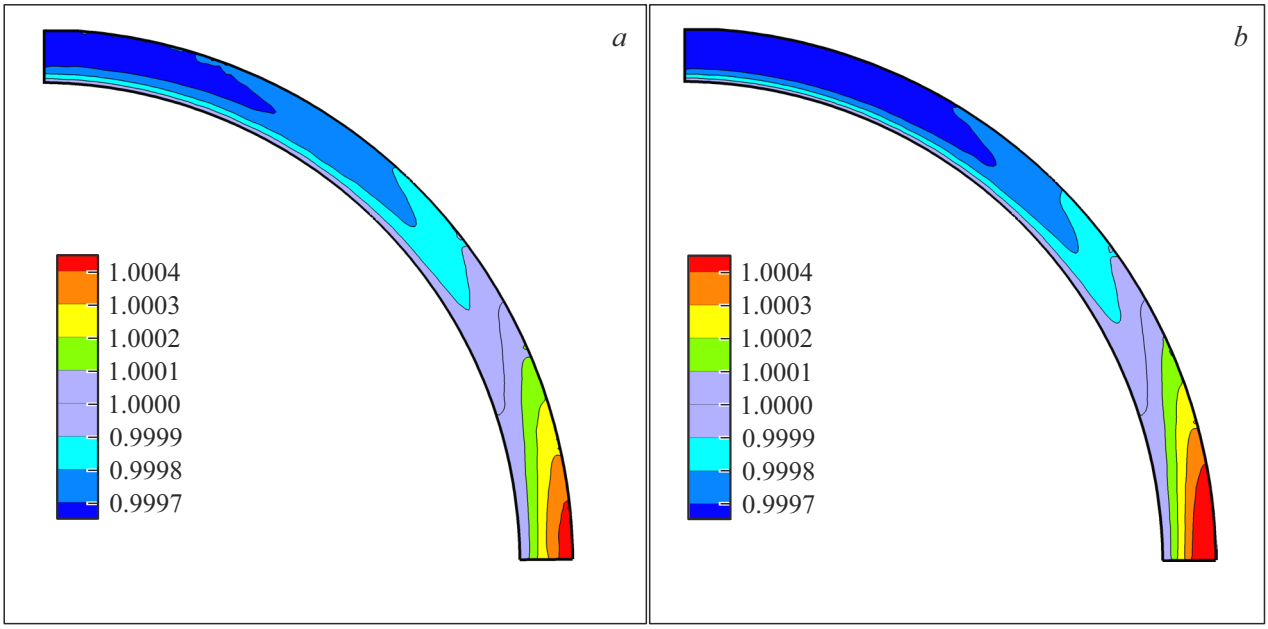

Figure 2. Distributions of the V values in the meridional plane of flow at $N = 0.04$, $\mathrm{Re}_1 = 1000$. $\alpha = 1$ (a) and 2 (b). A color version of the figure is provided in the online version of the paper.

similar: in a nearly vertical layer parallel to the rotation axis and adjacent to the inner sphere, the velocity changes are minimal. Velocity V decreases toward the rotation axis and the outer sphere and increases toward the equatorial plane and the outer sphere. Thus, the increase in velocity under the influence of noise becomes continuously less significant as one shifts along the meridional angle in the direction from the equator to the axis of rotation. At the same time, certain differences may also be noted: at $\alpha = 2$ (Fig. 2, b), the area of flow regions corresponding to the maximum change in velocity is larger than the one at $\alpha = 1$ (Fig. 2, a). Since the values of azimuthal velocity near the equatorial plane are an order of magnitude higher than in the polar region, the observed difference is indicative of a more intense generation of mean flows under the influence of noise with a higher spectral slope ($\alpha = 2$). This agrees completely with the earlier results for flows in wide layers driven by rotation of the boundaries in the same direction [9]: according to them, an increase in α leads to more intense generation of mean flows under the influence of noise.

In experiments [12] under stationary boundary conditions, the flow in a thin layer ($\delta = 0.1096$) became unstable with the formation of a pair of Taylor vortices near the equator at $\mathrm{Re}_{1c} = 1225$. No hysteresis was detected, and the Reynolds number determination accuracy was ± 12. In calculations [12] with the conditions of symmetry relative to the axis of rotation and the equator, $\mathrm{Re}_{1c} = 1225$ was also obtained, but only if finite perturbations were added. As is shown below, added perturbations reduce the calculated Re_{1c} values. According to calculations [13], the flow in layer $\delta = 0.11$ in the axisymmetric approximation remains stable up to $\mathrm{Re}_1 = 1500$. In three-dimensional calculations performed in the same study, Taylor vortices formed at $\mathrm{Re}_{1c} = 1262.2$, and the reverse transition occurred at 1261.1; the hysteresis magnitude was $d\mathrm{Re}_{1c} = 1.1$. The values of Re_{1c} and $d\mathrm{Re}_{1c}$ calculated in [13] decreased with an increase in the number of Legendre test functions in the meridional direction and the number of grid points in the radial direction.

In our calculations at $\delta = 0.11$, the flow instability was identified in the same way as in [15] (by the emergence of Taylor vortices in visualization of the azimuthal component of vorticity in the meridional flow plane; see Fig. 3):

$$\omega_\varphi = \frac{1}{rr'}\frac{\partial r u_\theta}{\partial r} - \frac{1}{r\theta'}\frac{\partial u_r}{\partial \theta}.$$

The value of $\mathrm{Re}_{1c} = 1263.5$, which agrees closely with the results reported in [13], was obtained in 3D calculations with stationary rotation without additional perturbations. In this case, the transition from the primary flow to Taylor vortices occurred without breaking the flow symmetry relative to the axis of rotation and the equator. Just as in [12], no hysteresis was observed ($d\mathrm{Re}_{1c} < 0.25$). The results of 2D ($\mathrm{Re}_{1c} = 1263.75$) and 3D calculations are almost identical; in all the examined cases, hysteresis was detected neither at $N = 0$, nor at $N \neq 0$. Thus, our calculations for stationary rotation produced the results that correspond in a number of parameters to the experimental and calculated data obtained earlier. This verifies the applicability of conditions of flow symmetry relative to the axis of rotation and the equator in these calculations. The dependence of the stability limit position on the type and amplitude of added noise was investigated further in 2D calculations. The flow was visualized using the velocity

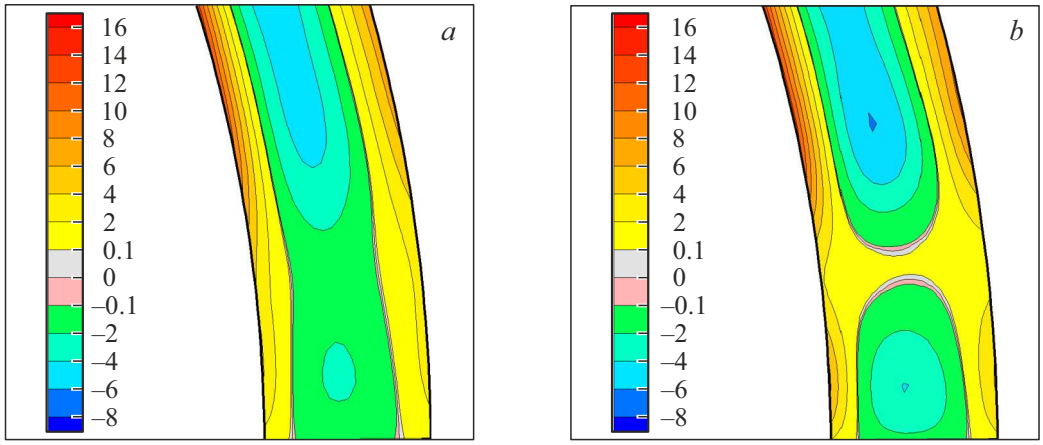

Figure 3. Distributions of the azimuthal component of vorticity in the meridional plane of flows at $\alpha = 1$ and $N = 0.06$. *a* — Primary flow (without Taylor vortices), $\mathrm{Re}_1 = 1220$; *b* — secondary flow after the loss of stability (with a Taylor vortex near the equatorial plane), $\mathrm{Re}_1 = 1258$. A color version of the figure is provided in the online version of the paper.

field averaged over 300 s. The dependence of Re_{1c} on the amplitude and type of noise is shown in Fig. 4. At Reynolds numbers above the stability limit for stationary rotation of the sphere (horizontal line in Fig. 4), the flow becomes unstable with respect to perturbations of an extremely small amplitude. At Reynolds numbers above the sloping curves (Fig. 4), the flow becomes unstable with respect to perturbations of rotation velocity of a finite amplitude. However, the transition to instability is „soft“ (features no hysteresis) in all the examined cases. Just as in the case with added „white“ noise ($\alpha = 0$) [10,11], an increase in N leads to a reduction in Re_{1c}. Compared to the data from [10,11], where Re_{1c} decreased by a few units at the most, the changes in Re_{1c} shown in Fig. 4 are considerably more profound. With noise amplitudes N being equal, the values of Re_{1c} at $\alpha = 2$ are significantly lower than those at $\alpha = 1$. Thus, the more intense generation of mean flows before the loss of stability at a higher slope of the $\Omega(t)$ spectrum leads to a reduction of critical Reynolds number values corresponding to the loss of stability.

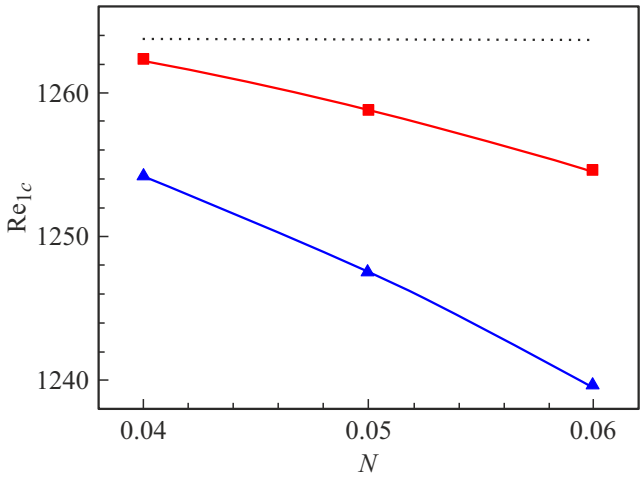

Figure 4. Dependences of the critical values of stability limit Re_{1c} on noise amplitude N at spectrum slope $\alpha = 1$ (squares) and 2 (triangles). The horizontal line corresponds to stationary rotation of the boundaries.

Funding

This study was supported by a grant from the Russian Science Foundation (project No. 25-27-00044).

Conflict of interest

The authors declare that they have no conflict of interest.

References

[1] W. Horsthemke, R. Lefever, *Noise-induced transitions* (Springer, Berlin, 1984).
[2] T. Morita, T. Omori, Y. Nakayama, S. Toyabe, T. Ishikava, Phys. Rev. E, **101**, 063101 (2020). DOI: 10.1103/PhysRevE.101.063101
[3] Yu.G. Markov, I.N. Sinitsyn, Dokl. Phys., **54** (7), 350 (2009). DOI: 10.1134/S1028335809070118.
[4] G. Smadja, Y. Copin, W. Hillerbrandt, C. Saunders, C. Tao, Astron. Astrophys., **682**, A121 (2024). DOI: 10.1051/0004-6361/202245497
[5] M. Schroeder, *Fractals, chaos, power laws: minutes from an infinite paradise* (Dover Publ., N.Y., 1991).
[6] Y. Xu, R. Gu, H. Zhang, W. Xu, J. Duan, Phys. Rev. E, **83**, 056215 (2011). DOI: 10.1103/PhysRevE.83.056215
[7] L.B. Ryashko, A.N. Pisarchik, Phil. Trans. Roy. Soc. A, **380**, 20200313 (2022). DOI: 10.1098/rsta.2020.0313
[8] D.Yu. Zhilenko, O.E. Krivonosova, Tech. Phys. Lett., **49** (4), 62 (2023). DOI: 10.21883/TPL.2023.04.55881.19506.
[9] D.Yu. Zhilenko, O.E. Krivonosova, Tech. Phys., **69** (2), 179 (2024).
[10] D.Yu. Zhilenko, O.E. Krivonosova, Tech. Phys., **66** (6), 903 (2021). DOI: 10.1134/S1063784221060232.

[11] D.Yu. Zhilenko, O.E. Krivonosova, Tech. Phys., **67** (5), 376 (2022). DOI: 10.1134/S1063784222060093.
[12] Yu.N. Belyaev, I.M. Yavorskaya, in *Itogi nauki i tekhniki*. Ser. Mekhanika zhidkosti i gaza (VINITI, M., 1980), Vol. 15, pp. 3–80 (in Russian).
[13] O. Zikanov, J. Fluid Mech., **310**, 293 (1996). DOI: 10.1017/S0022112096001814
[14] A.J. Youd, C.F. Barenghi, Phys. Rev. E, **72**, 056321 (2005). DOI: 10.1103/PhysRevE.72.056321
[15] D.Yu. Zhilenko, O.E. Krivonosova, Tech. Phys. Lett., **44** (6), 457 (2018). DOI: 10.1134/S1063785018060147.
[16] M.H. Choujaa, M. Riahi, S. Aniss, Phys. Fluids, **36**, 014101 (2024). DOI: 10.1063/5.0178263
[17] N. Nikitin, J. Comp. Phys., **217**, 759 (2006). DOI: 10.1016/j.jcp.2006.01.036
[18] K.E. Abdul'manov, N.V. Nikitin, Fluid Dyn., **57** (5), 571 (2022). DOI: 10.1134/S0015462822050093.

Translated by D.Safin